AIChE WILEY InterScience DISCOVER SOMETHING GREAT

MATERIALS, INTERFACES, AND ELECTROCHEMICAL PHENOMENA

Hydrothermal Synthesis of Mesoporous Materials from Diatomaceous Earth

Zhenzi Jing, Hirotaka Maeda, Koji Ioku, and Emile H. Ishida
Graduate School of Environmental Studies, Tohoku University, Aoba-ku 980-8579, Japan

DOI 10.1002/aic.11235
Published online June 28, 2007 in Wiley InterScience (www.interscience.wiley.com).

Hydrothermal synthesis of mesoporous materials from diatomaceous earth has been carried out under saturated steam pressure (0.2–1.56 MPa) at 393–473 K for up to 72 h by slaked lime introduction. During the hydrothermal synthesis process, calcium silicate hydrate (CSH) was among the first phase formed and invariably appeared before tobermorite. The CSH formation seemed to exert a positive effect on the strength development and pore size evolution initially; whilst the tobermorite formation appeared to further enhance the strength and narrow the pore size. With curing at 473 K for 18 h, both of the strength and pore size distribution tended to reach optimal at which the pore size distribution also ranges between mesoporous area (2–50 nm in diameter). The highest strength seemed to coincide with the finest pore size distribution of the synthesized porous material during hydrothermal processing in this study.
 AIChE J, 53: 2114–2122, 2007
Keywords: hydrothermal synthesis, mesoporous materials, diatomaceous earth, tensile strength, pore distribution

Introduction

Diatomaceous earth (DE), a siliceous, sedimentary rock consisting principally of the fossilized diatom skeletal, is an attractive and adequate material that offers a great application in industry owing to its unique properties of low bulk density, high porosity with strong adsorbability, chemically inert in most liquids, and gases and thermal resistance.[1–4]

Mesoporous materials, on the other hand, have extensively been applied in many processes such as catalysts, adsorbents, molecular sieves, and sensors[5,6] because of their excellent properties of high specific surface area and narrow pore size (2–50 nm in diameter). The mesoporous materials used as building materials also showed to have capability both of eliminating volatile organic compounds (VOCs)[7,8] and of regulating indoor humidity by their porous bodies.[9] The requirement to obtain mesopores with a controlled pore size has therefore become more and more important for many practical applications.

Synthesis of mesoporous materials from DE has attracted widely attention. The DE mesoporous material should possess the properties both of the mesoporous materials and of DE. For example, if the DE mesoporous material could be used as a building material, it will possess the properties not only of extremely lightweight and heat insulation like DE, but also of regulating-humidity and eliminating-VOCs like mesoporous materials. To utilize effectively the inherent porous properties of DE, the DE porous materials are usually manufacture at a relative low firing temperature (1073–1173 K). The low firing temperature and introduction of porosity will inevitably degrade the mechanical properties of porous materials, and thus limit the range of its applications. Ishida[9] further reported that the manufacture temperature of earthen products must be lower than 773 K to sustain their inherent properties (porous properties) and performance of earthen materials.

A hydrothermal processing method has been applied to the field of the manufacture of calcium silicate products and solidification of wastes into building materials.[10–14] The

Correspondence concerning this article should be addressed to Z. Jing at zzjing@hotmail.com.

hydrothermal processing method is usually carried out at 423–473 K in saturated steam pressure, and therefore it might be suitable to manufacture DE mesoporous materials so as to sustain the inherent properties of DE.

In hydration of Portland cement,[15,16] hydrothermal curing calcium silicate products and hydrothermal solidification of inorganic wastes,[10–14] tobermorite has been shown to be the most important strength-producing constituent. A tough mesoporous material from DE, therefore, may be synthesized hydrothermally with tobermorite formation.

To the best of our knowledge, however, there seems to be few published work dealing with hydrothermal synthesis of mesoporous materials from DE, and the relationship between the strength and the porous structure (pore size distribution) has not been adequately described to date.

The objective of the present work is to experimentally investigate the effects of slaked lime addition, compaction pressure, curing time and curing temperature on the strength development, and pore size evolution of the synthesized specimens. In particular, the relationship between the strength development and pore size evolution is examined in order to find out how to synthesize a tough mesoporous material from DE. The results are expected to provide practical information on manufacture of the DE porous materials, which should be useful in the use of the materials as adsorbents, catalyst, humidity-regulating materials and similar applications.

Experimental

Materials

Pre-calcined (1473 K) DE powder, obtained from Showa Chemical Industry, Japan, was used for the synthesis of porous material because of the fact that the raw DE frequently contains an important rate of impurities that can restrain its efficiency in many applications.[17] Reagent-grade slaked lime from Wako Pure Chemical Industries, Japan, was used as an additive. The chemical composition of DE was determined by X-ray fluorescence (XRF) (Model RIX3100, Rigaku), the particle size distributions of DE and slaked lime used were measured by laser diffraction technology (Model X100, Microtrac) and DE crystalline morphology was observed by a scanning electron microscope (SEM) (Model S-4100, Hitachi).

Specimen synthesis

DE mixed with slaked lime at different mixing ratio was used as starting material. The starting material (15 g) was first mixed manually in a mortar with 30 mass % distilled water (4.5 mL), and then the mixture was compacted into a column-shaped mold (30 mm diameter $\times$ 120 mm height) by compaction pressure of 5–30 MPa. The demolded specimens (30 mm diameter $\times$ 20 mm height) were subsequently autoclaved under saturated steam pressure (0.2–1.55 MPa) at 393–473 K, for up to 72 h. The Teflon (PTFE) lined stainless steel hydrothermal apparatus showed in Figure 1 was used for curing the demolded specimens. After autoclaving, all the synthesized specimens were dried at 353 K for 24 h before testing.

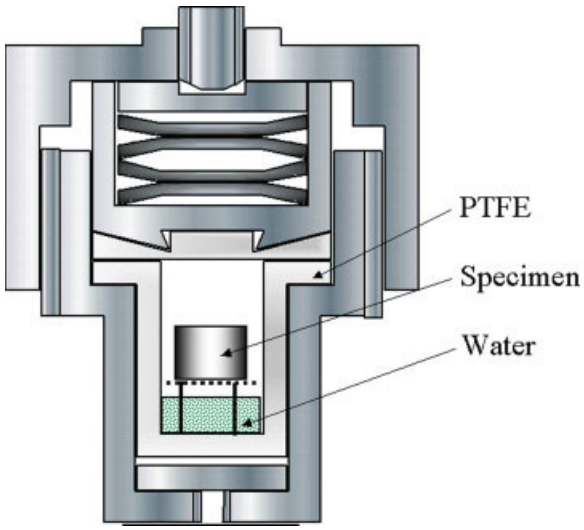

Figure 1. Hydrothermal apparatus used for curing compacted specimens.

[Color figure can be viewed in the online issue, which is available at www.interscience.wiley.com.]

Analyses

Once dried, the synthesized specimens (30 mm diameter $\times$ 20 mm height) were used to measure the tensile strength using the Brazilian testing method.[18] The Brazilian tests were performed in a universal testing machine (Model M1185, Instron) at a crosshead speed of 0.2 mm/min. The measured maximum load (P_{max}) was substituted into the following equation to calculate the tensile strength (σ_t):

$$\sigma_t = 2P_{max}/\pi dt$$

where d is the specimen diameter (in this case, $d = 30$ mm) and t is the specimen thickness (in this case, $t = 20$ mm). All tensile strength measurements presented in this study are the average of at least three specimens. After Brazilian testing, the crushed specimens were investigated using several techniques: for crystalline phase analysis, X-ray diffraction (XRD) (Model MiniFlex, Rigaku), for microstructure, SEM, and for pore size distribution, mercury intrusion porosimetry (MIP) (Model Poremaster 33P, Quantachrome).

Results

Material characterization

The particle size distributions of the DE and slaked lime are shown in Figure 2, in which the particle size of slaked lime is much smaller than that of DE. SEM photograph shown in Figure 3 reveals that the disk-shaped diatoms are still well preserved even after pre-calcined at 1473 K, and numerous inherent voids visible ($\sim$0.2 μm in diameter) range regularly on the disk-shaped diatoms.

The chemical composition of DE presented in Table 1 shows that SiO_2 content occupies more than 86 mass %, whilst CaO is only less than 1.0 mass %.

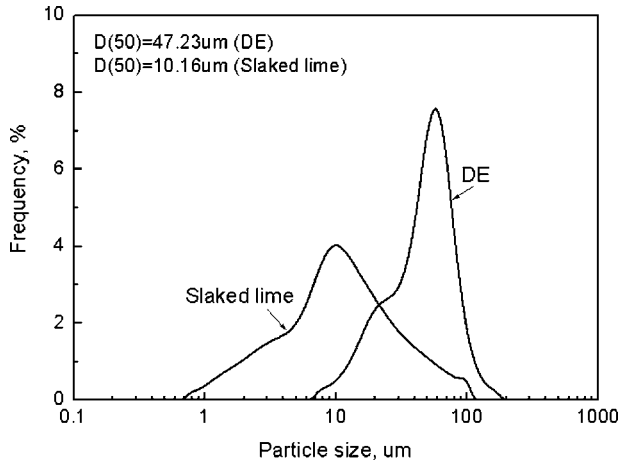

Figure 2. Particle size distributions of the DE and slaked lime used. D(50) means 50% of the particles are smaller than this value (μm).

Tensile strength

The tensile strength development of the specimens mixed with slaked lime up to 60 mass %, cured at 473 K for 12 h and compacted by 20 MPa is shown in Figure 4, and the CaO/SiO_2 molar ratio (C/S) in the starting materials is also plotted in this figure. The tensile strength increases with increasing slaked lime content up to 50 mass %, and then decreases for the larger slaked lime content, indicating that an optimum slaked lime content exists for the hydrothermal synthesis of DE. The tensile strength at slaked lime content of 50 mass % reaches more than 10 MPa, which is higher than ordinary concrete. The slaked lime addition of 50 mass %, thereby, was used throughout this study since then.

The changes in the tensile strength of the specimens compacted by different compaction pressures and cured at 473 K for 12 h are given in Figure 5. The tensile strength increases with increasing compaction pressure up to 20 MPa, and then gives the almost constant value for the larger compaction pressure. Since then, the compaction pressure of 20 MPa was used throughout this study.

Table 1. Composition of DE Used (mass %)

SiO_2	86.4
CaO	0.9
Al_2O_3	9.2
TiO_2	0.3
Fe_2O_3	2.5
K_2O	0.7
Ignition loss	2.0

The tensile strength development for the specimens cured at 473 K during the autoclave process was investigated. As shown in Figure 6, the tensile strength markedly increases up to autoclave curing of 18 h, developing the ultimate tensile strength of more than 10 MPa, which is 10 times higher than that without curing. After 18 h, the strength sharply drops with curing time until 24 h to less than 8 MPa; beyond this it tends to decline gradually until autoclave curing time up to 72 h.

The tensile strength evolution for the specimens cured at different curing temperatures for 12 h is shown in Figure 7. The tensile strength increases markedly with curing temperature, developing the tensile strength of more than 6 MPa at 393 K. After 393 K, the strength increases gradually until 423 K, and then it tends to increase significantly again to 473 K.

XRD results

XRD analyses were also carried out on these specimens with different slaked lime additions, curing times and curing temperatures discussed above.

The mineralogical composition of DE identified from XRD, as shown in Figure 8, corresponds mainly to critobalite (SiO_2), and a small proportion of hematite (Fe_2O_3), quartz (SiO_2), and kyanite (Al_2SiO_5). With addition of slaked lime,

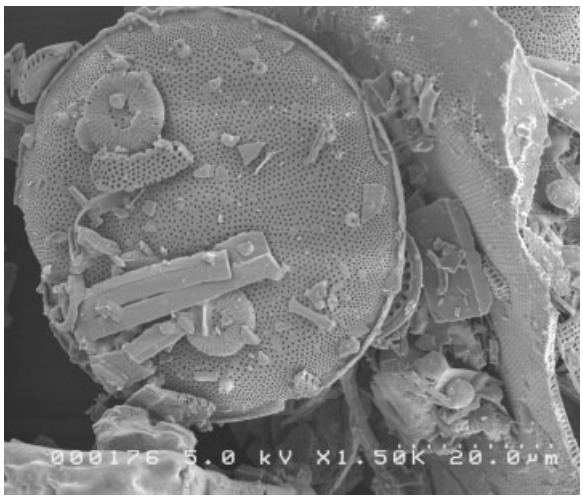

Figure 3. Scanning electron microscopy (SEM) micrograph of the DE used.

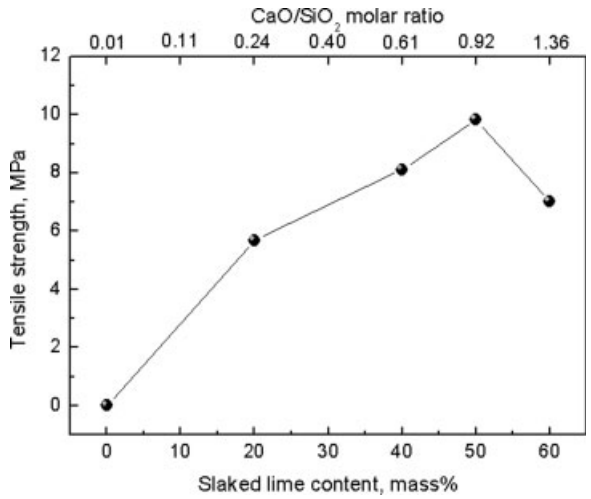

Figure 4. Effect of slaked lime content on tensile strength of specimens compacted by 20 MPa, and cured at 473 K for 12 h.

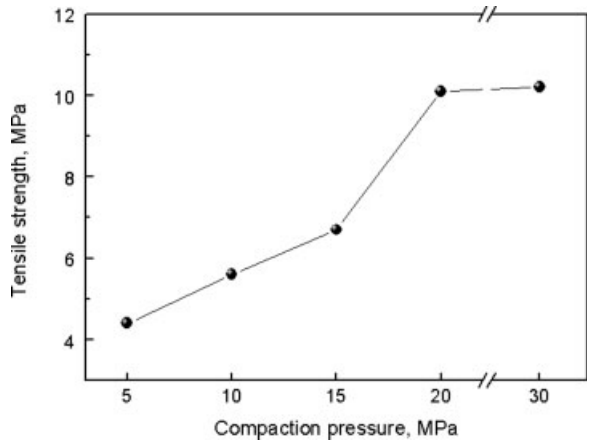

Figure 5. Effect of compaction pressure on tensile strength of specimens cured at 473 K for 12 h.

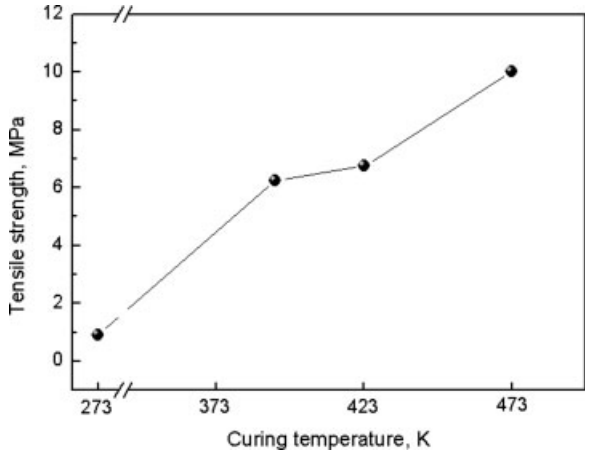

Figure 7. Effect of curing temperature on tensile strength of specimens cured for 12 h.

the peak intensities of critobalite and quartz at slaked lime of 20 mass % appear to decrease significantly and at the same time the peak characteristic of calcium silicate hydrate (CSH) gels tends to form. Above slaked lime of 40 mass %, a new phase corresponding to 1.1 nm tobermorite ($Ca_5(OH)_2Si_6O_{16}{\cdot}4H_2O$) forms and a trace of portlandite phase ($Ca(OH)_2$) becomes distinct, accompanying a marked reduction in the peak intensities of critobalite and quartz. The peak intensities of tobermorite and portlandite formed appear to increase with increasing slaked lime introduction.

The phase evolution with curing time is shown in Figure 9. The main mineralogical compositions corresponding to portlandite, critobalite, and quartz for the specimen without curing (0 h) are confirmed. From curing time of 1 h, a trace of the peak corresponding to CSH tends to be distinct and its peak intensity increases with increasing curing time up to 6 h, indicating that the longer the curing time, the more the CSH formed. A new phase corresponding to 1.1 nm tobermorite tends to form from 12 h, and its peak intensity also increases for the longer curing time.

Figure 10 shows the phase evolution with curing temperature. The peak intensities of portlandite and critobalite decrease gradually with increasing curing temperature. During 393–423 K, a trace of peak corresponding to CSH gel tends to appear, and at 473 K, another new phase of 1.1 nm tobermorite is observed.

SEM results

The microstructure evolution of the specimens cured at 473 K for different curing times is shown in Figure 11. SEM micrographs reveal that different curing times have resulted in different morphologic crystals formed within the specimen cured for 0, 3, 12, and 24 h.

Pore size distribution

A detailed investigation of the microstructure evolution of the specimens with different slaked lime introduction, compaction pressure, curing time, and curing temperature was also conducted by measuring the pore size distribution.

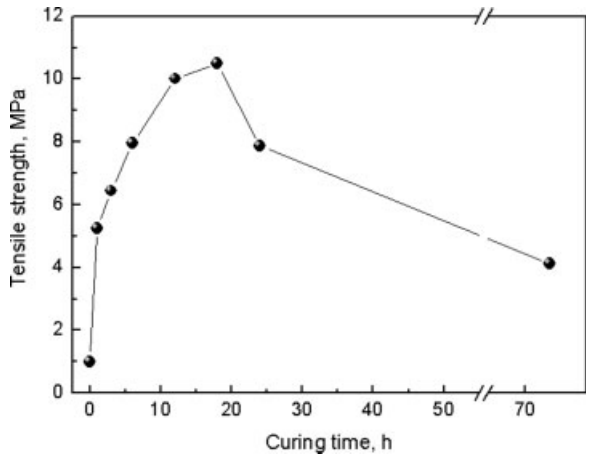

Figure 6. Effect of curing time on tensile strength of specimens cured at 473 K.

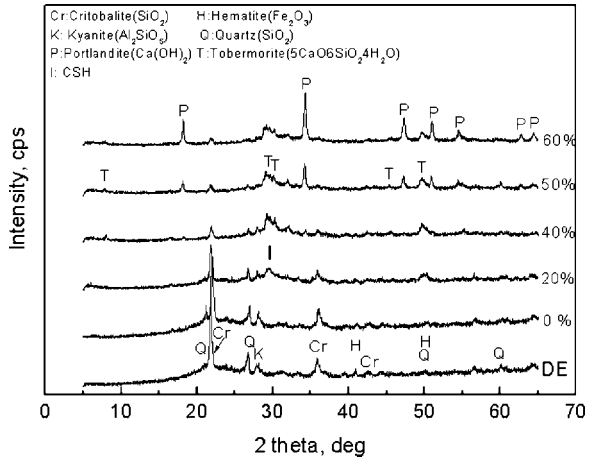

Figure 8. XRD patterns of specimens compacted by 20 MPa, and cured at 473 K for 12 h with different slaked lime additions.

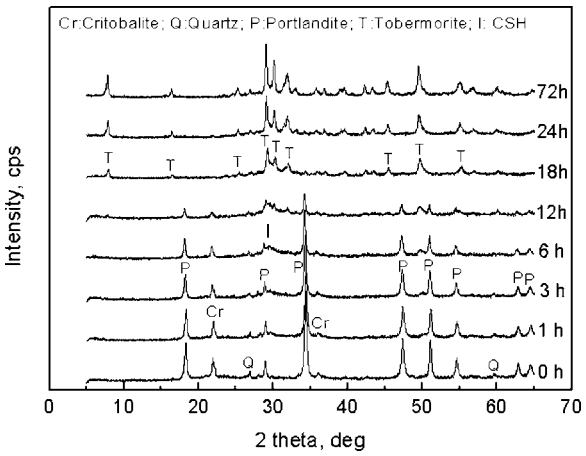

Figure 9. XRD patterns of specimens cured at 473 K for different curing times.

Without slaked lime addition (0 mass %), the pore diameter distribution shown in Figure 12 gives the highest frequency peak at 2.5 μm in diameter, and another peak at 0.2 μm. For slaked lime content of 20 mass %, the main peak tends to shift toward a finer diameter (from 2.5 to 0.6 μm), and at the same time a new peak at $\sim$0.04 μm forms. With increasing slaked lime introduction, the initial main peak of pore distribution tends to disappear, and another new peak at 0.015 μm in diameter forms from slaked lime content of 40 mass %.

Figure 13 illustrates the evolution of the pore size distributions of the specimens with different compaction pressures. The pore size distribution at compaction pressure of 5 MPa shows the highest frequency of pore distribution peak at 5 μm, and some other main peaks also at 0.015 and 0.5 μm. With increasing compaction pressure up to 30 MPa, in addition to the peaks at 0.015 in diameter still keeping their position, the highest peak (at 5 μm) tends to disappear and the peak at 0.5 μm shifts to 0.03 μm.

Figure 14 reveals the microstructure evolution of the specimens cured at 473 K for different curing times. Before hydrothermal treatment (curing time of 0 h), the pore diameter distribution gives the highest frequency peak at 0.9 μm. With increasing curing time, the peak tends to shift toward a finer pore distribution (0.02 μm) until 18 h; beyond this, however, the peak shift back to 0.3 μm up to 72 h.

The changes in the pore size distribution with different curing temperatures (Figure 15) indicate that the pore size distribution peak tends to shift toward a finer pore size with increasing curing temperature and at 473 K a new peak at 0.015 μm forms.

Discussion

The objective of the present work is to investigate the effects of slaked lime introduction, compaction pressure, autoclave curing time and curing temperature on the strength development, and pore size distribution and to elucidate the relationship between the strength development and pore size distribution of synthesized specimens from DE.

Effect of slaked lime introduction

The composition of DE used in this study shows that SiO_2 content (86.4%) is much higher than CaO content (0.9%). To enhance the strength of synthesized specimens, slaked lime was introduced to form tobermorite. The tensile strength (Figure 4), as expected, increased with increasing slaked lime content up to 50 mass %, and then decreased afterwards. It is noted that the C/S of starting material at the optimum slaked lime content of 50 mass % (0.92) is close to the C/S of tobermorite (0.83), suggesting that the strength development may be due to tobermorite formation.

XRD analysis (Figure 8), carried out on these specimens with different slaked lime additions, revealed the relationship between the phase evolution and strength development. The main mineralogical compositions corresponding to critobalite, hematite, quartz, and kyanite without slaked lime addition (0 mass %) were confirmed. At slaked lime contents of 20 and 40 mass %, new peak characteristics of calcium silicate hydrate (CSH) gel and 1.1 nm tobermorite ($Ca_5(OH)_2$-$Si_6O_{16}\cdot 4H_2O$) tended to form, respectively. At slaked lime of 60 mass %, however, a peak of portlandite became high because of more slaked lime introduction. Comparison between the XRD results and strength development indicates that with slaked lime addition, the initial strength development is due mainly to CSH formation, whilst further strength enhancement seems to be responsible for tobermorite formation. However, a decrease in strength takes place because of the excessive slaked lime (60 mass %) added. For the relationship between C/S and crystal formation, a low C/S ($\sim$0.24) favors CSH formation, and a high one (>0.61) promotes tobermorite formation. The observation is in accordance with remark[19] that the C/S conditions the rate of formed CSH transformation to tobermorite for the reaction between silica fume and kaolin. The excess of portlandite formation caused by slaked lime introduction (60 mass %) appears to act inhibitory for the hydrothermal reaction between DE and slaked lime, thus leading to a strength reduction, which is in agreement with outcomes,[20,21] that extensive surrounding of fly ash particles by calcium hydroxide resulted in a substantial limitation of the reactivity of the particles, and is also observed in a similar case of hydrothermal solidification of coal fly ash.[22]

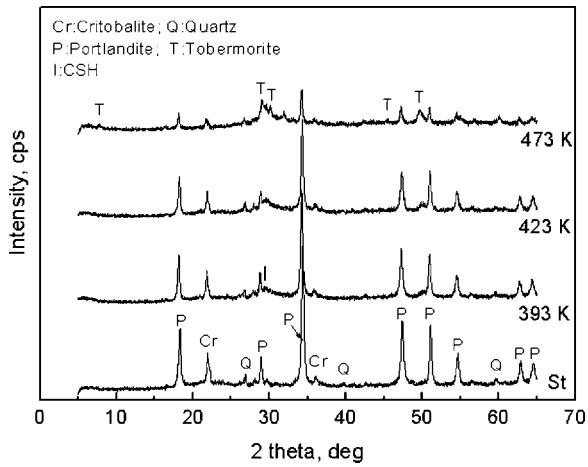

Figure 10. XRD patterns of specimens cured at different curing temperatures for 12 h.

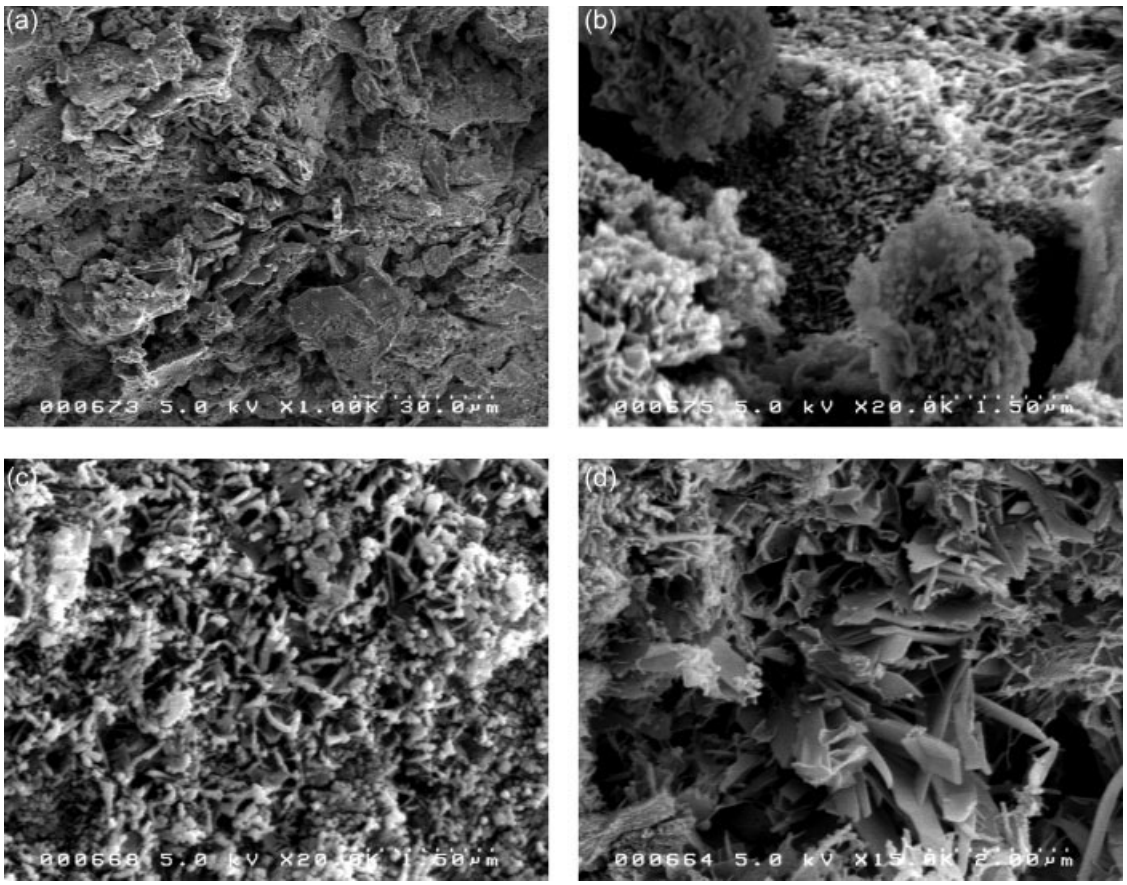

Figure 11. SEM micrographs of the specimens cured at 473 K, for (a) 0 h, (b) 3 h, (c) 12 h, and (d) 24 h.

CSH gel and tobermorite formations are expected to affect the pore size distribution. The pore size distribution at slaked lime of 0 mass % (Figure 12) gave the highest frequency peak at 2.5 μm and another peak at 0.2 μm in diameter, which should correspond to the spaces between the DE particles within the specimen and the inherent voids of DE (Figure 3), respectively. At slaked lime content of 20 mass %, the main peak (at 2.5 μm) tended to shift toward a finer diameter, and synchronously a new peak (~0.04 μm) formed. These peaks may correspond to the space dimensions between the particles

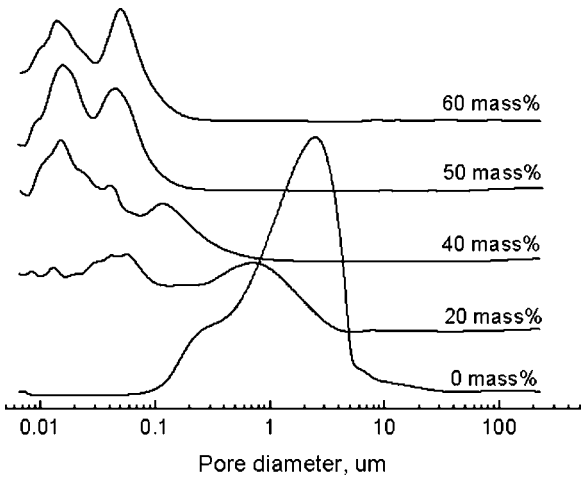

Figure 12. Evolution of pore size distribution of specimens compacted by 20 MPa, and cured at 473 K for 12 h with different slaked lime additions.

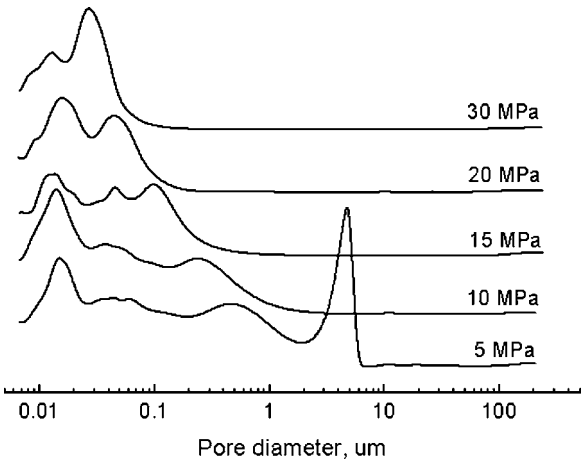

Figure 13. Evolution of pore distribution of specimens cured at 473 K for 12 h with different compaction pressures.

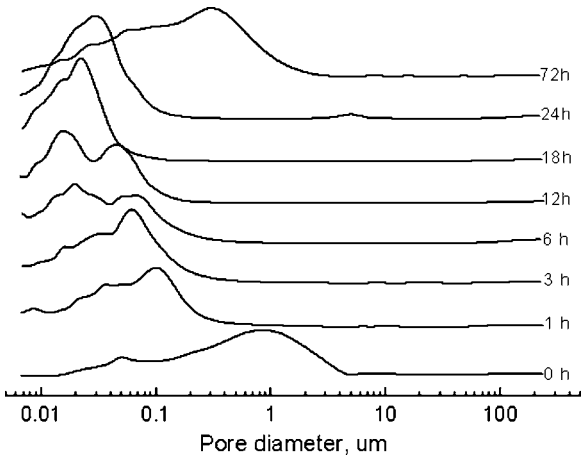

Figure 14. Evolution of pore distribution of specimens cured at 473 K for different curing times.

at the time their formation, and the peak shift and formation suggest the formation of some crystals, which results in a change in pore dimension. According to the XRD results (Figure 8), the newly formed crystals consist mainly of CSH, indicating that the new peak at 0.04 μm corresponds to the intercrystalline pores of CSH gel, and the formed CSH filling into (decreasing) the spaces between DE particles has led to the peak shift from 2.5 to 0.6 μm. With increasing slaked lime content up to 60 mass %, the initial main peak of pore distribution between DE particles tended to disappear, suggesting that these pores might have been filled up with formed crystals. From slaked lime content of 40 mass %, another new peak at 0.015 μm in diameter formed. The newly formed pores (0.006–0.03 μm in diameter) at the slaked lime addition of 50 mass % can be observed by the SEM micrograph shown in Figure 11c, in which the platy crystals form, and their intercrystalline pores are filled with numerous individual fine crystal particles. From the XRD results (Figure 8), the platy crystal should be 1.1 nm tobermorite and the fine particle, a concomitant phase formed with the introduction of slaked lime 40–60 mass %, should mainly be portlandite precipitated. Consequently, the intercrystalline voids of formed tobermorite and interspaces between the individual fine particles may correspond to the peaks at 0.04 and 0.015 μm, respectively, between slaked lime addition of 40–60 mass %. With increasing slaked lime addition, the pore size tends to become finer (pore size distribution shifts toward the finer pore size) because of the accelerating effect of slaked lime on the rate of hydrothermal reaction (more crystals formed), which might result in a denser matrix, thus promoting the strength development shown in Figure 4.

Effect of compaction pressure

In hydrothermal processing, starting material was first compacted and then the as-compacted specimens were cured in an autoclave. The compaction pressure, therefore, is expected to affect the strength development and pore size distribution of the specimens. The tensile strength (Figure 5), as expected, increased until compaction pressure of 20 MPa, and then gave the almost constant value afterwards. A higher compaction pressure will lead to a denser as-compacted specimen, and a close contact of particles within specimen may be favorable to the hydrothermal reaction, thus enhancing the strength. Above 20 MPa, however, the increase in the tensile strength becomes very slow, suggesting that further compaction pressure has little effect on the strength development.

The compaction pressure also affects the pore size distribution of the specimens. For the pore size distribution (Figure 13) at 5 MPa, the highest frequency of pore distribution peak at 5 μm in diameter might correspond to the initial spaces between DE particles and other main peaks at 0.015 and 0.5 μm might be due to crystal formation within the specimen. With increasing compaction pressure up to 30 MPa, the highest peak at 5 μm tended to disappear and the peak at 0.5 μm shifted to 0.03 μm, whilst the peaks at 0.015 in diameter appeared to keep their positions. The former is due probably to the fact that a higher compaction pressure results in a denser matrix (narrower pores), and the narrower pores within the specimen can be filled up readily with the formed crystals. SEM micrograph of the specimen compacted by 20 MPa shown in Figure 11c revealed that the peaks at 0.015 and 0.045 μm correspond to the interspaces of fine individual portlandite particles precipitated and intercrystalline spaces of tobermorite formed, respectively. The peak shifted from 0.5 to 0.03 μm, however, might be responsible for the crystal (tobermorite) growth. It is well known that crystal growth depends strongly on its growth space, i.e., a narrower space favors to form finer crystals. With increasing compaction pressure, the specimen becomes denser, and the denser specimen (finer spaces between particles) is favorable to finer crystal (tobermorite) formation, thus leading to finer intercrystalline pores formed.

Effect of curing time

The tensile strength development (Figure 6) of the specimens cured at 473 K for different autoclave curing times showed that the strength markedly increases up to autoclave curing of 18 h, and then tends to decline gradually afterwards. XRD analyses (Figure 9) revealed the phase evolution

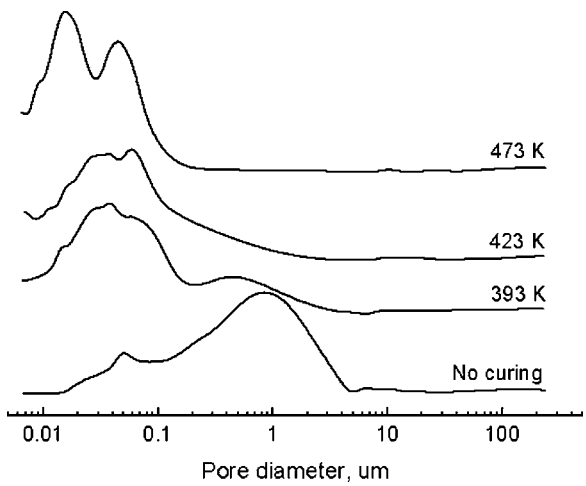

Figure 15. Evolution of pore distribution of specimens cured at different curing temperatures for 12 h.

during this process. From 1 h, a trace of the peak corresponding to CSH becomes distinct and the peak intensity increases with increasing curing time up to 6 h, indicating that the longer the curing time, the more the CSH formed. Comparison between the phase evolution and strength development with different curing times shows that the CSH formation contributes significantly to the initial strength development, and the more the CSH gel formed, the higher the strength. Another new phase corresponding to 1.1 nm tobermorite becomes distinct at 12 h, and its peak intensity increases for the longer curing time. As mentioned earlier, the C/S conditions the type of calcium silicate hydrate products formed (CSH or tobermorite). This result indicates that even for a larger C/S (0.92), a shorter curing time appears to be favorable to CSH formation, while a longer one promotes tobermorite formation. During initial hydrothermal process, the amount silica and calcium dissolved from the starting material is relatively low, and the low amount of silica and calcium may favor the CSH formation. With increasing curing time, the higher concentrations of silica and calcium appear to promote tobermorite formation. It should be noted that at curing time of 18 h, almost all portlandite, critobalite, and quartz have been consumed to form tobermorite. Compared with the strength development (Figure 6), this behavior demonstrates that the tobermorite formed seems to further promote the strength development of the specimen; however, even tobermorite formed, an excessive curing time (>24 h) appears to exert a negative influence on the strength development.

The strength development may be affected by the microstructure evolution (Figure 14) of the specimens for different curing times. The pore diameter distribution at curing time of 0 h gave the highest frequency peak at 0.9 μm. This initial pores seem to have a finer pore distribution than that without slaked lime addition (Figure 12) because of the introduction of the finer slaked lime powders (Figure 2). According to the SEM micrograph of the specimen without curing (0 h) shown in Figure 11a, the peak corresponds mainly to the initial spaces between DE particles. With increasing curing time, the pore size distribution tended to shift. According to the XRD results (Figure 9), for curing time of 3 h, the peak at 0.05 μm mainly corresponded to the CSH gel formation. SEM micrograph (Figure 11b) verified the CSH gel formation, where its sponge-like morphology seems to possess intercrystalline pores of $\sim$0.05 μm in diameter. It is noted that in addition to the peak formation at 0.05 μm, another new peak at 0.02 μm appears to be observed from curing time of 6 h. SEM micrograph of the specimen cured at 12 h (Figure 11c) showed that the peak at $\sim$0.02 μm should be due mainly to the interspaces between the accumulation of the portlandite particles, and the peak at 0.04 μm should result from tobermorite formation. Undoubtedly, the interlocked structure between the platy tobermorite filling with finer portlandite particles has resulted in a matrix that is denser and homogeneous, thus enhancing the strength. Note that the finest pore distribution is obtained at curing time of 18 h, at which its pore diameter distribution ranges wholly within mesoporous area (2–50 nm). Increasing curing time favors the crystal formation, thus a denser crystal formed resulting in the finest pore distribution. The hydrothermal process can be considered as a dissolution/precipitation process, and a long curing time may result in crystal growth. SEM micrograph of the specimen cured for 24 h (Figure 11d) showed large crystals formed, with few fine portlandite particles precipitated. According to the XRD result (Figure 9), the crystal phase was 1.1 nm tobermorite. The large tobermorite, which possesses large intercrystalline pores filling up with few portlandite particles, may probably be the outcome of the strength reduction shown in Figure 6. From the evolution of pore size distribution peaks with increasing curing time, although the peak corresponding to CSH or/and tobermorite formation shifts greatly (toward a finer or an larger pore size), the peak of the pore size distribution due to the accumulation of the portlandite particles appears to keep its position always at $\sim$0.015 μm (during 6–18 h), which shows that the pore size distribution may depend mainly on the tobermorite or CSH crystallization. At 72 h, the peak of pore size distribution shifts back to 0.3 μm in diameter, which suggests that the formed tobermorite has become very large (large intercrystalline pores), and this sparse crystal matrix may lead to the strength reduction. It is notable that at 18 h the finest pore size distribution has resulted in the highest strength development. This also suggests that the toughest hydrothermally synthesized specimen from DE seems to coincide with the finest pore size distribution.

Effect of curing temperature

The curing temperatures also affect the strength development and pore size distribution. After curing (Figure 7), the tensile strength at 393 K markedly increased, and became gradual until 423 K, and then tended to increase significantly again up to 473 K.

The strength enhancement was found to depend on the phase changes. Figure 10 showed that the peak intensities of portlandite and critobalite decrease gradually with increasing curing temperature, reflecting a development of hydrothermal reaction between the slaked lime and DE. During 393–423 K, a trace of peak corresponding to CSH gel tended to appear, which is believed to enhance the initial strength. At 473 K, a new phase corresponding to 1.1 nm tobermorite was observed, which results in the almost highest tensile strength. During this process, for a high C/S (0.92) used, the curing temperature also conditions the type of calcium silicate hydrate products (CSH or tobermorite), and a low curing temperature (e.g. <423 K) seems to be unfavorable to tobermorite formation.

The crystal formation (CSH and tobermorite) also made the pore size distribution peak (Figure 15) shift toward a finer pore size. From SEM micrograph of the specimen cured at 473 K (Figure 11c), the peak at 0.015 μm in diameter was due to the fine portlandite particle formation. The strength development shown in Figure 7 seems to have a close relation with the pore size evolution (microstructure change). A similar pore size distribution between 393 and 423 K seems to result in a similar strength development (393–423 K). The platy structure of tobermorite formed at 473 K, which is filled with the portlandite particle formation, is believed to improve the strength development.

Conclusions

To utilize the inherent properties (porous properties) of DE effectively, hydrothermal synthesis of mesoporous material from DE has been carried out under saturated steam pressure

(0.2–1.56 MPa) at 393–473 K for up to 72 h by introduction of slaked lime. The effects of (1) slaked lime addition, (2) compaction pressure, (3) curing time, and (4) curing temperature on the strength development and pore size distribution of the specimens were investigated to find out how to synthesize a tough mesoporous material from DE. From the above investigation the following main conclusions may be drawn:

1. The slaked lime addition exerted an accelerative effect on the hydrothermal reaction between slaked lime and DE. The strength development and pore size evolution seemed to depend on the C/S of starting material. A low C/S ($\sim$0.24) appeared to favor the CSH formation, and a high one ($>$0.61) seemed to promote tobermorite formation; whilst the excessive addition of slaked lime (C/S $\geq$ 1.36) appeared to act inhibitory for tobermorite formation. With slaked lime addition, the more crystal (CSH or tobermorite) formation resulted in a denser matrix (finer pore size distribution), thus enhancing the strength of the synthesized specimens.

2. The compaction pressure seemed to significantly affect the strength development and pore size distribution. A higher compaction pressure resulted in a denser as-compression specimen. The denser matrix appeared to have capability of both promoting the hydrothermal reaction between particles and favoring a finer crystal (a finer pore) formation, thus enhancing the strength.

3. During hydrothermal process, the crystal formation seemed to condition the strength development and pore size distribution. CSH was among the first phase formed and invariably appeared before tobermorite. The CSH formed exerted a positive effect on the strength development and pore size distribution initially; whilst the tobermorite formed filling with fine portlandite particles appeared to further enhance the strength and narrow the pore size. At curing time of 18 h, the pore size distribution tended to become finest, and its pore size distribution ranged also between mesoporous area (2–50 nm). However, excessive curing time ($>$24 h) seemed to cause the crystal overgrowth, thus resulting in a larger crystal formed and a decrease in the strength. The toughest specimen cured at 473 K for 18 h in this study appeared to coincide with the finest pore size distribution, which is very useful for us to obtain simultaneously both high strength and fine pore size.

4. The curing temperature affected significantly the hydrothermal reaction between slaked lime and DE. A high curing temperature appeared to favor more crystal formation, in turn, exerting a positive influence on the strength development and pore size distribution. CSH formation at lower curing temperature ($<$423 K) led to the initial strength development and pore size distribution; whilst the tobermorite formation at high curing temperature (473 K) seemed to further improve the strength development and narrow pore size.

Acknowledgments

The work reported here was supported by the Grant-in-Aid for Scientific Research for Japan Society for the Promotion of Science (No. 18201014).

Literature Cited

1. Rutherford SW, Coons JE. Water sorption in silicone foam containing diatomaceous earth. *J Colloid Interface Sci*. 2007;306:228–240.
2. Martinovic S, Vlahovic M, Boljanac T, Pavlovic L. Preparation of filter aids based on diatomites. *Int J Miner Process*. 2006;80:255–260.
3. Athanassion CG, Kavallieratos NG, Meletsis CM. Insecticidal effect of three diatomaceous earth formulations, applied alone or in combination, against three stored-product beetle species on wheat and maize. *J Stored Prod Res*. 2006;doi:10.1016/j.jspr.2006.08.004.
4. Fukumizu H, Yokoyama S, Kitamura K. Study on a new humidity controlling material porous soil "allophane"—design of humidity controlling material. *Resour Process*. 2005;52:128–135 (in Japanese).
5. Zhang L, Ying JY. Synthesis and characterization of mesoporous niobium-doped silica molecular. *AIChE J*. 1997;43:2793–2801.
6. Endo A, Inagi Y, Fujisaki S, Yamamoto T, Ohmori T, Nakaiwa M. Simple and rapid synthesis of mesoporous silica by vacuum solvent evaporation. *AIChE J*. 2006;52:1275–1277.
7. Sinha AK, Suzuki K. Novel mesoporous chromium oxide for VOCs elimination. *Appl Catal B Environ*. 2007;70:417–422.
8. Yang X, Chen Q. A coupled airflow and source/sink model for simulating indoor VOCs exposures. *Indoor Air*. 2001;11:257–269.
9. Ishida EH. Soil-ceramics (Earth), self-adjustment of humidity and temperature. In: Schwartz M, editor. *Encyclopedia of Smart Materials*. New York: Wiley, 2002;1015–1029.
10. Gutovic M, Klimesch DS, Ray A. Strength development in autoclaved blends made with OPC and clay-brick waste. *Constr Build Mater*. 2005;19:353–358.
11. Zheng QJ, Wang W. Calcium silicate based high efficiency thermal insulation. *Br Ceram Trans*. 2000;99:187–190.
12. Jing Z, Matsuoka N, Jin F, Hashida T, Yamasaki N. Municipal incineration bottom ash treatment using hydrothermal solidification. *Waste Manage*. 2007;27:287–293.
13. Jing Z, Ishida H, Jin F, Hashida T, Yamasaki N. Influence of quartz particle size on hydrothermal solidification of blast furnace slag. *Ind Eng Chem Res*. 2006;45:7470–7474.
14. Schuur HML. Calcium silicate products with crushed building and demolition waste. *J Mater Civil Eng*. 2000;12:282–287.
15. Yudenfeund M, Hannz KM, Skalny J, Odler I, Brunauer S. Hardened portland cement pastes of low porosity. V. Compressive strength. *Cement Concrete Res*. 1972;2:731–743.
16. Brunauer S, Skalny J, Odler I, Yudenfreund M. Hardened portland cement pastes of low porosity. VII. Further remarks about early hydration. Composition and surface area of tobermorite gel. Summary. *Cement Concrete Res*. 1973;3:279–293.
17. Bamda B, Kessaissia Z, Donnet JB, Wang TK. Analytical study of the variation of physico-chemical and structural properties of a Kieselguhr during its decarbonation. *Analusis*. 1998;26:164–169.
18. International Society for Rock Mechanics Commission on Standardization of laboratory and Field Tests. Suggested methods for determining tensile strength of rock materials. *Int J Rock Mech Min Sci Geomech Abstr*. 1978;15:99–103.
19. Mostafa NY, El-Hemaly SAS, Al-Wakeel EI, El-Korashy SA. Activity of silica fume and dealuminated kaolin at different temperatures. *Cement Concrete Res*. 2001;31:905–911.
20. Antiohos S, Papageorgiou A, Tsimas S. Activation of fly ash cementations systems in the presence of quicklime, Part 2: Nature of hydration products, porosity and microstructure development. *Cement Concrete Res*. 2006;36:2123–2131.
21. Grutzeck MW, Roy DM, Scheetz BE. Microstructure of high-lime fly ash cementitious mixes. *Cement Concrete Res*. 1981;11:291–294.
22. Jing Z, Matsuoka N, Jin F, Yamasaki N, Suzuki K, Hashida T. Solidification of coal fly ash using hydrothermal processing method. *J Mater Sci*. 2006;41:1579–1584.

Manuscript received Feb. 26, 2007, and revision received May 19, 2007.